Noise analysis of BDS coordinate time series based on dynamic positioning

Jun Ma[1], Chengdu Cao[1], Yang Min[1], Lv Zhou[2]

[1] China Railway Siyuan Survey And Design Group Co., LTD, Wuchang District, Wuhan City, Hubei Province, 430063, China, (794598508@qq.com,yangzhiqou.student@sina.com, 165570976@qq.com)

[2] College of Geomatics and Geoinformation, Guilin University of Technology, Guilin, 541004, China, (zhoulv_whu@163.com)

Key words: *BDS*; *dynamic positioning*; *deformation monitoring*; *coordinate time series*; *colored noise*

ABSTRACT

At present, most of the deformation monitoring research based on BDS (BeiDou Navigation Satellite System) ignores the influence of colored noise in the coordinate time series of station, which is not conducive to obtaining accurate deformation speed, and may lead to an erroneous analysis of deformation results. In the real-time deformation monitoring using BDS dynamic positioning technology, in order to analyze the colored noise in the BDS coordinate time series and its influence in this mode, This study selects 2 days of observations from two pairs of short baseline stations located in various locations in Australia. The noise amplitudes and accuracy of deformation velocity in BDS, Global Positioning System (GPS), and GPS/BDS coordinate time series are analyzed on the basis of white noise (WN) + power law (PL) noise combination model. Results show that the BDS coordinate time series in the dynamic positioning mode contains colored noise (including spurious periodic signals), and ignoring its influence will lead to an overly optimistic evaluation of the deformation monitoring results. Moreover, using GPS/BDS technology for deformation monitoring will weaken the false periodic signal caused by error, thereby reducing the influence of colored noise and improving the accuracy of deformation velocity estimations.

I. INTRODUCTION

With the continuous improvement of the BDS and the extension of research, the BDS can locate with a high precision, and its coordinate time series can be applied to high-precision deformation monitoring. Colored noise may be included in BDS coordinate time series due to system errors and geophysical effects. For high-precision real-time deformation monitoring, such as dam deformation, bridge vibration, and slope slip, considering the influence of colored noise helps to obtain an accurate deformation velocity and improve the level of deformation monitoring. Therefore, analyzing the colored noise in the BDS coordinate time series has become an important part of BDS high-precision deformation monitoring.

At present, some scholars have carried out deformation monitoring research based on BDS/GPS technology. Jiang et al.(2016) show that the BDS deformation monitoring accuracy in mid-latitude regions is better than that in high latitudes. Xiao et al. (2016) studied the deformation monitoring algorithm with millimeter level precision based on BDS. The results show that the precision of short baselines derived from BDS is better than 1 mm for the horizontal components, better than 2 mm for the vertical components. Using integrated GPS and BDS data processing with post-installation residual editing and SNR-based stochastic model strategies, Xi et al. (2018a) effectively manage the effects of satellite signal blockage and multipath effects to obtain reliable dynamic deformation monitoring information for bridges. Xi et al.(2018b) proposed a rapid initialization method with triple-frequency BDS and GPS observations. In addition, Gong et al.(2017) also proposed a rapid phase ambiguity resolution method to shorten the initial or re-convergence time based on GPS/BDS multi-frequency observables. Although the above research results are rich, they mostly focus on a multipath effect, noise-weakening method, and data-processing strategy to improve the accuracy of a baseline solution. When estimating the deformation velocity in accordance with the deformation time series, the existence of colored noise is neglected, thereby seriously affecting the accuracy of deformation monitoring results and leading to an incorrect explanation of the cause of deformation. Therefore, this study uses the BDS coordinate time series of two pairs of stations in Australia as an example to analyze the variation in deformation velocity accuracy before and after considering the colored noise in the dynamic positioning mode. The periodic signals and noise in BDS, GPS, and GPS/BDS coordinate time series are also compared.

II. EXPERIMENTAL DATA AND NOISE ESTIMATION METHODS

A. *Experimental data*

The second-generation BDS can only cover the Asia Pacific region and cannot provide location services to users worldwide. Therefore, this study selects the CUT0 and CUTC stations at the top of the Curtin University Business School building in Australia and the YAR3 and YARR stations in the city of Dongara in Western Australia. The CUT0 and YAR3 stations are used as the corresponding monitoring stations.

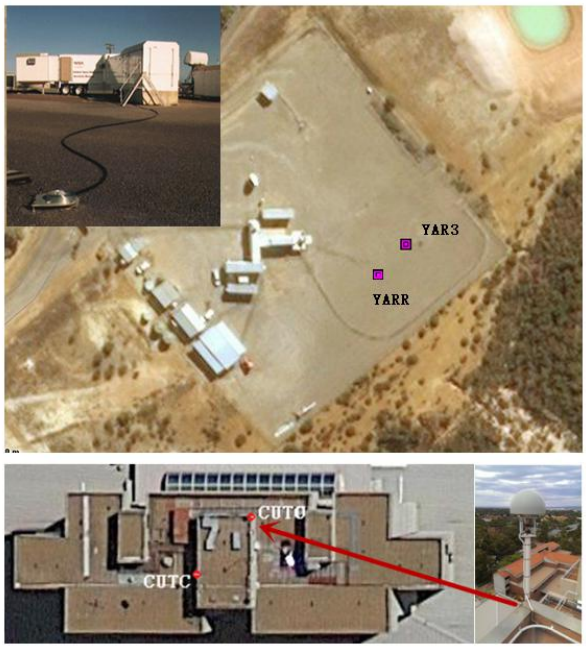

Figure 1. Specific locations of the CUT0, CUTC, YAR3, and YARR station

It can be seen from Fig. 1 that the distances between the monitoring and reference station does not exceed 30 m. The observation data of the BDS dual frequency from April 10–11, 2018, are selected, and the satellite cutoff height angle is 15°. The sampling interval is 30 s, and each station has 5760 epochs. In a dynamic positioning mode, the ambiguity is fixed through the LAMBDA method, and the E, N, and U coordinates of each station are estimated by extended Kalman filter algorithm. Before analyzing the noise in BDS coordinate time series, a triple-error method is used to eliminate gross errors, and the clean BDS coordinate time series are finally obtained.

B. *Noise estimation method*

WN + PL noise combination model is extensively used in the noise analysis of coordinate time series. The covariance matrix of the observed values in the noise model is presented as follows:

$$\mathrm{D(y)} = \sigma_w^2 I + \sigma_K^2 Q_K \quad (1)$$

where y is the coordinate time series of the single component of a station; D(y) is the covariance matrix; K is the spectral index of PL noise; σ_w^2 and σ_K^2 are the variances of white and power law noises, respectively; and Q_K is the co-factor matrix of PL noise related to the spectral index (Williams *et al.*, 2008; Langbein *et al.*, 2012). Under the WN + PL noise combination model, the most commonly used noise estimation method is the maximum likelihood estimation method. The joint probability density of the residual v and the covariance matrix of the coordinate sequence are expressed as follows:

$$\mathrm{lik}(\mathrm{v},Q_y) = \frac{1}{(2\pi)^{N/2}(\det Q_y)^{1/2}} \exp\left(-0.5 v^T Q_y^{-1} v\right) \quad (2)$$

The use of the logarithm of both sides of Equation (2) yields

$$\ln\left[\mathrm{lik}(\mathrm{v},Q_y)\right] = -0.5\left[\ln(\det Q_y) + v^T Q_y^{-1} v + N\ln(2\pi)\right] \quad (3)$$

According to the principle of maximum likelihood estimation, various combinations of white and colored noises will obtain different maximum likelihood logarithmic values. A large value indicates a reliable result. The specific process of estimating noise using this method will not be described here, but the readers may refer to the related literature (Bos *et al.*, 2008)

III. Experimental results

A. *Power spectrum and noise estimation*

The double logarithmic power spectrum of WN tends to stabilize, that is, the spectral index is 0, and the spectral index of colored noise is not 0. Therefore, an important basis for judging whether a coordinate time series contains colored noise is the spectral index of the double log power spectrum of its residual sequence. Before analyzing the power spectrum, the BDS coordinate time series of the monitoring station CUTC and the YARR station are analyzed. In Fig. 2, the residual is larger in the CUTC station than in the YARR station. The reference station is near the monitoring station; thus, the influences of the receiver clock error, satellite ephemeris error, troposphere, and ionospheric delay are basically eliminated by a double-difference mode. The coordinate time series of the two stations are mainly affected by the multipath effect. Fig. 1 illustrates the specific locations of the two stations and their surrounding environment. The CUTC and CUT0 stations are located at the highest point of the roof and at a certain distance from the ground and roof. The monument of the YARR station is steel plate and close to the ground, and the surroundings are relatively flat. Therefore, the multipath effect is more severe in the CUTC station than in the YARR station. Also, the monuments of the CUTO and CUTC stations are steel mask with a length of 2 meters. These monuments mounted on the roof are likely to be affected by wind loads. The above factors are likely to result in the residual being greater in the CUTC station than in the YARR.

The coordinate time series of the two stations contain periodic signals, and the periodic signals are more characterized in the YARR station than in the CUTC station, especially the periodic signals in the U component. The selected observation data have a short span; consequently, the coordinate time series does not reflect the long-term periodic motion of the station. The periodic signal in the BDS coordinate time series of the YARR station may be a false signal caused by an error (Xixiu et al., 2012; Yang et al., 2016). The YARR station is slightly affected by the multipath effect,

and the periodic characteristics of the coordinate time series are remarkable. Thus, the cause of its periodic signal may be related to the BDS system error. The CUTC station is increasingly affected by the multipath effect, and therefore, the residual seriously affects the periodic signal.

When considering only linear trends, the spurious periodic signals will be treated as noises and behave as colored noises. In Fig. 3, the spectral indices of the power spectra of the BDS coordinate time series of the CUTC and YARR stations are all less than 0 and greater than −1, and the spectral index of the CUTC is the smallest. This result indicates that the short-term BDS coordinate time series of both stations contain colored noises.

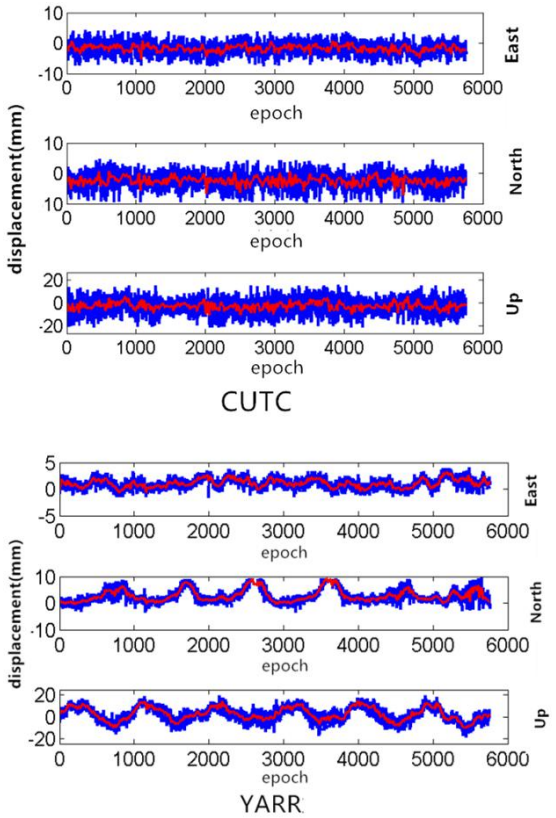

Figure 2. CUTC and YARR station BDS coordinate time series; the blue curve represents the original coordinate time series, and the red curve represents the sequence extracted by the original coordinate time series after wavelet transform processing

Table 1 Estimations of noise amplitudes after considering the colored noise.

Station	Component	K	PL(mm•d$^{(K/4)}$)	WN(mm)
CUTC	E	-0.9	3.1	1.5
	N	-0.7	4.3	1.5
	U	-0.8	9.1	4.9
YARR	E	-1.7	2.9	1.1
	N	-1.7	1.4	0.5
	U	-1.7	6.8	3.1

On the basis of the WN + PL noise combination model, the noise amplitude (standard deviation) estimations (Table 1 and 2) and the standard deviations of deformation velocity estimations are calculated through the maximum likelihood estimation method to analyze the influence of colored noise on the deformation velocity accuracy (Table 3). K represents the spectral index of PL noise in Table 1. As can be seen from Table 1, based on the WN + PL noise model, the amplitude estimates of WN are less than that of colored noises. This result shows that colored noise still dominates in the noise of the BDS coordinate time series. Comparing Table 1 with Table 2, the estimations of the noise amplitudes are different from the former in case of considering only WN and are smaller than those of the colored noise. As shown in Table 3, when only WN is considered, the standard deviation (STD) of the velocity estimate are smaller than that in the WN + PL noise combination model. Accordingly, ignoring colored noise will result in an erroneous estimation of the noise amplitude, thus leading to an overly optimistic assessment of the accuracy of the deformation velocity estimate.

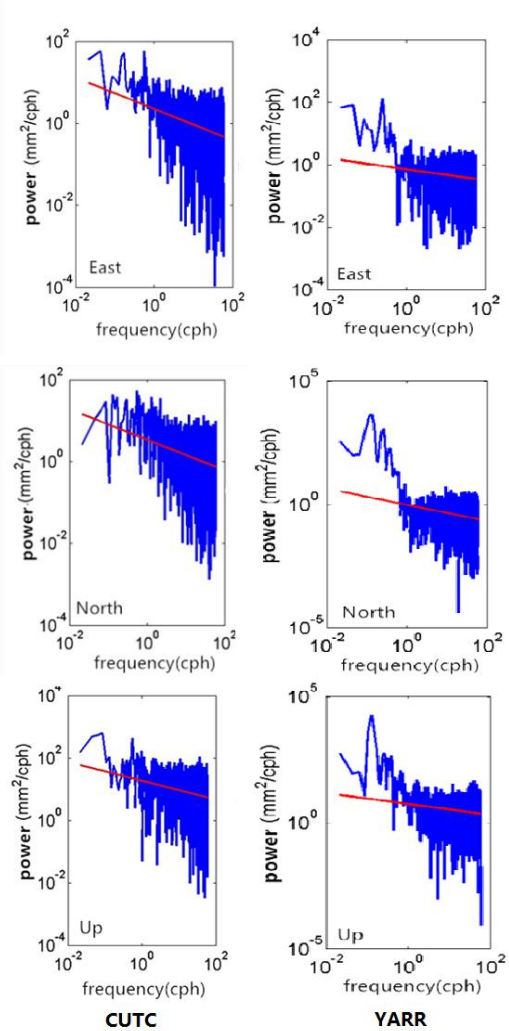

Figure 3. Double logarithmic power spectrum of the BDS coordinate time series of the CUTC and YARR stations and their fitting straight lines

Table 2 Estimations of noise amplitudes before considering the colored noise.

Station	Component	WN(mm)
CUTC	E	1.9
	N	2.3
	U	6.1
YARR	E	2.5
	N	0.9
	U	6.6

Table 3 STD of velocity estimations before after considering the colored noise (mm)

Station	Component	WN model	PL model
CUTC	E	0.05	0.5
	N	0.06	0.5
	U	0.14	1.15
YARR	E	0.06	3.55
	N	0.02	1.77
	U	0.15	8.33

B. *Comparison of the noises in the BDS, GPS, and GPS/BDS coordinate time series*

In addition to GPS technology, the GPS/BDS technology is extensively used for deformation monitoring. However, analyzing a coordinate time series obtained in accordance with the abovementioned technique also ignores the influence of colored noise. To compare the noise in the BDS, GPS, GPS/BDS coordinate time series in the dynamic positioning mode, the GPS and GPS/BDS coordinate time series and the power spectra of the abovementioned stations are obtained on the basis of the same observation data and data-processing strategy (Fig. 4). Wavelet transform method is used to nearly denoise the coordinate time series (Fig. 5). In Fig. 5, for the CUTC station, the waveform results of the BDS, GPS, and GPS/BDS coordinate time series are substantially the same, and the amplitude is smaller in the GPS/BDS coordinate time series than that in the BDS and GPS. For the YARR station, the time series in the three components exhibit clear periodic characteristics, in which the periods of BDS and GPS/BDS coordinate time series are relatively consistent, and the GPS coordinate time series contains additional periodic signals. The periodic signals of the GPS and BDS coordinate time series have the largest amplitude in the E and N components, correspondingly. This result indicates that the factors that cause the periodic signal in the YARR coordinate time series are independent of the geophysical environment in which the station is located and are related to the satellite positioning system. Table 4 lists the standard deviations in the three components of the two stations based on different positioning systems. The standard deviation is substantially smaller in the GPS/BDS coordinate time series than in the BDS and GPS coordinate time series. This difference may be due to that additional effective satellites can be observed using both positioning systems, and solution accuracy is increasingly precise. Therefore, the GPS/BDS technology can be used to effectively reduce the effects of noise in deformation monitoring.

Table 4 Standard deviations (mm) of the BDS, GPS, and GPS/BDS coordinate time series

Component	BDS		GPS		GPS/BDS	
	CUTC	YARR	CUTC	YARR	CUTC	YARRA
E	1.91	0.94	2.07	2.05	1.43	1.12
N	2.34	2.51	2.35	1.54	1.63	1.27
U	6.12	6.71	5.55	6.35	4.00	5.34

Table 5 Noise amplitude estimations of GPS coordinate time series and standard deviations of velocity estimations

Station	Component	K	PL(mm•d$^{(K/4)}$)	WN(mm)
CUTC	E	-0.6	4.4	0.4
	N	-0.5	4.9	0.1
	U	-0.5	11.4	0.1
YARR	E	-1.7	4.1	0.6
	N	-1.7	4.1	0.5
	U	-1.7	15.8	2.24

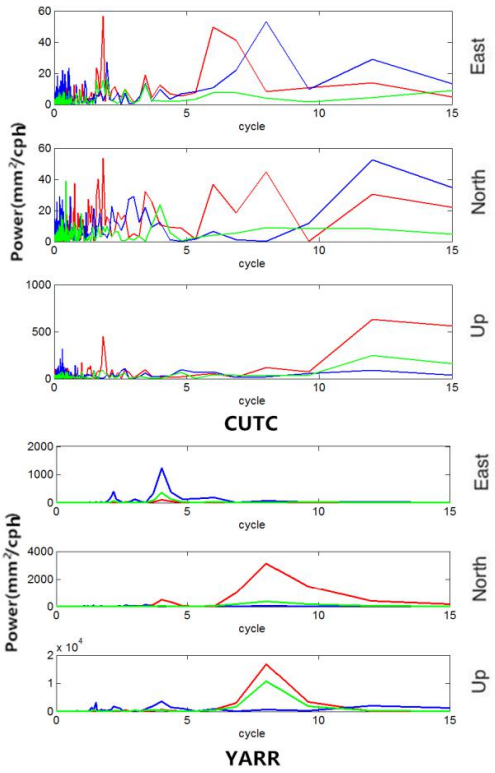

Figure 4. Power spectrum of the CUTC and YARR station coordinate time series. The red, blue, and green curves correspond to the power spectra of the BDS, GPS, and GPS/BDS coordinate time series

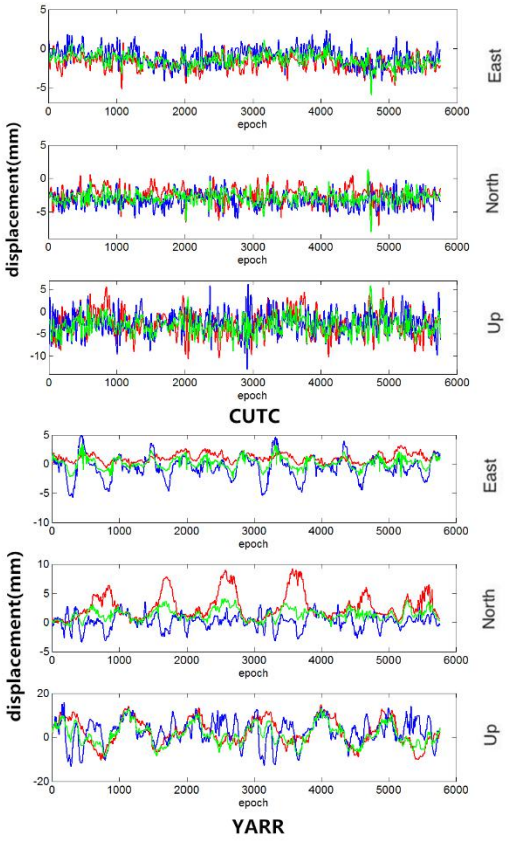

Figure 5. Curves of the CUTC and YARR station coordinate time series after wavelet denoising. The red, blue, and green curves represent the BDS, GPS, and GPS/BDS coordinate time series, respectively

Table 6 Noise amplitude estimations of GPS/BDS coordinate time series and standard deviations of velocity estimations

Station	Component	K	PL(mm•d$^{(K/4)}$)	WN(mm)
CUTC	E	-0.6	3.7	0.3
	N	-0.7	2.9	0.6
	U	-0.6	7.5	2.3
YARR	E	-1.2	2.7	0.6
	N	-1.1	2.72	0.2
	U	-1.7	7.9	2.3

Table 7 STD of velocity estimations

Station	Component	GPS	GPS/BDS
CUTC	E	0.3	0.3
	N	0.3	0.3
	U	0.7	0.7
YARR	E	3.4	1
	N	5.1	0.7
	U	19.5	9.7

Fig. 4 demonstrates that the BDS, GPS, and GPS/BDS time series of each component of the CUTC station contain many signals with different periods. Section 3.1 indicates that these periodic signals may be false signals caused by multipath effects. Overall, the power is less in the GPS/BDS coordinate time series than in the BDS and GPS coordinate time series. For the YARR station that is slightly affected by multipath effects, the coordinate time series mainly contain false signals with periods of 4 and 8 h. For signals with a period of 4 h, the GPS coordinate time series has the highest power in the E and U components. For signals with a period of 8 h, the BDS coordinate time series have the highest power in the N and U components. The powers of the two periodic signals in the GPS/BDS coordinate time series are between those in the BDS and GPS coordinate time series. Therefore, using GPS and BDS for deformation monitoring simultaneously helps reduce the false periodic signal caused by systematic errors.

To quantify the colored noise in the three types of coordinate time series, on the basis of the WN + PL noise model, the maximum likelihood estimation method is used to obtain the estimations of the noise amplitudes (Table 5 and Table 6) in the GPS and GPS/BDS coordinate time series and the standard deviations (Table 7) of the velocity estimates of the two stations. A comparison of Tables 1 and 5 implies that the WN amplitudes are larger in the BDS coordinate time series than in the GPS coordinate time series. Moreover, WN is associated with the satellite system because the station and receiver are the same. And the WN amplitude estimates in the GPS/BDS coordinate time series are between those in the BDS and GPS coordinate time series, whereas the PL noise is smaller than that for the BDS and GPS. As shown in Table 7, the standard deviations of velocity estimates for GPS/BDS are also smaller than those for GPS and BDS. This result shows that deformation monitoring can achieve more accurate deformation results using the GPS/BDS technology than using only the GPS or BDS technology.

IV. Conclusion

Two pairs of short baseline stations are used as examples, and the colored noise of the BDS coordinate time series in a dynamic positioning mode is analyzed and compared with those in the GPS and GPS/BDS coordinate time series. The results show that the error caused by the multipath effect and systematic error of BDS in the dynamic positioning mode can lead to spurious periodic signals in the BDS coordinate time series. These spurious signals behave as colored noises and dominate the noise when only linear trends are considered. Ignoring the effects of colored noise will make the assessment of the accuracy of the deformation velocity estimate increasingly optimistic. The use of GPS/BDS technology for deformation monitoring helps weaken false cycle signals, thereby reducing the effect of colored noise and effectively

improving the accuracy of deformation monitoring results.

V. Acknowledgements

This research is supported by the research project of China Railway Siyuan Survey And Design Group Co., LTD (Contract No 2018K134), the Postdoctoral Innovation Post in Hubei Province in 2018, the Foundation of Guilin University of Technology (Grant No. GUTQDJJ2018036), and Natural Science Foundation of Guangxi (Grant No. 2018GXNSFBA050006).

References

Jiang, W., Xi, R., Chen, H., & Xiao, Y. (2017). Accuracy analysis of continuous deformation monitoring using BeiDou Navigation Satellite System at middle and high latitudes in China. *Advances in Space Research*, 59(3), 843-857.

Yugang, X., Weiping, J., Hua, C., Peng, Y., & Ruijie, X. (2016). Research and Realization of Deformation Monitoring Algorithm with Millimeter Level Precision Based on BeiDou Navigation Satellite System. *Acta Geodaetica et Cartographica Sinica*, 45(1), 16-21.

Xi, R., Chen, H., Meng, X., Jiang, W., & Chen, Q. (2018a). Reliable Dynamic Monitoring of Bridges with Integrated GPS and BeiDou. *Journal of Surveying Engineering*, 144(4), 04018008.

Xi, R., Jiang, W., Meng, X., Zhou, X., & He, Q. (2018b). Rapid initialization method in real-time deformation monitoring of bridges with triple-frequency BDS and GPS measurements. *Advances in Space Research*.

Gong, X., Lou, Y., Liu, W., Zheng, F., Gu, S., & Wang, H. (2017). Rapid ambiguity resolution over medium-to-long baselines based on GPS/BDS multi-frequency observables. *Advances in Space Research*, 59(3), 794-803.

Williams, S. D. (2008). CATS: GPS coordinate time series analysis software. *GPS solutions*, 12(2), 147-153.

Langbein, J. (2012). Estimating rate uncertainty with maximum likelihood: differences between power-law and flicker–random-walk models. *Journal of Geodesy*, 86(9), 775-783.

Bos, M. S., Fernandes, R. M. S., Williams, S. D. P., & Bastos, L. (2008). Fast error analysis of continuous GPS observations. *Journal of Geodesy*, 82(3), 157-166.

Xixiu, W., (2012). GPS multipath effect systematic error research based on incremental kalman filter. *Engineering of Surveying & Mapping*, 21(6), 35-37.

Yang, H., Yang, X., Sun, B., & Su, H. (2016). Global Navigation Satellite System multipath mitigation using a wave-absorbing shield. *Sensors*, 16(8), 1332.